

Optical Engineering

SPIDigitalLibrary.org/oe

Enhanced fractional Fourier lens with isotropic transformation media

Xiangyang Lu
Jin Hu
Ran Tao

Enhanced fractional Fourier lens with isotropic transformation media

Xiangyang Lu,^{a,b} Jin Hu,^a and Ran Tao^a

^aBeijing Institute of Technology, School of Information and Electronics, Beijing 100081, China

^bZhongyuan University of Technology, School of Electronic and Information Engineering, Zhengzhou 450007, China

E-mail: bithj@bit.edu.cn

Abstract. By manipulating the principal stretches during a two-step space mapping within the framework of transformation optics, the input spatial frequency bandwidth of a conventional Fourier lens can be extended based on an isotropic transformation material. Isotropy is important for easy fabrication, low loss, and broadband application; moreover, it suggests a route for realizing Fourier transforms of continuous fractional order with enhanced input spatial frequency bandwidth. © The Authors. Published by SPIE under a Creative Commons Attribution 3.0 Unported License. Distribution or reproduction of this work in whole or in part requires full attribution of the original publication, including its DOI. [DOI: [10.1117/1.OE.52.6.060501](https://doi.org/10.1117/1.OE.52.6.060501)]

Subject terms: transformation optics; conformal mapping; graded index; fractional Fourier transform.

Paper 130062L received Jan. 15, 2013; revised manuscript received Apr. 11, 2013; accepted for publication May 2, 2013; published online Jun. 3, 2013.

Of late, considerable attention has been paid to the transformation method,¹⁻³ because it provides an intuitive and direct way of designing interesting materials that can control electromagnetic,¹⁻³ acoustic,⁴ and elastic⁵ wave propagation at will. Many interesting devices, such as invisible cloaks,^{2,3} have been designed based on transformation method. This method has also been explored to improve optical information processing. Li et al.⁶ designed a Fourier lens that has wider input spatial frequency bandwidth by applying transformation optics to the conventional graded index (GRIN) lens. Their result, however, depended on an anisotropic material, which can usually be realized with local resonant mechanism or metamaterial technology,² and is challenging for low-loss and broadband applications. For example, the lens constructed by Li et al.⁶ can only work in a particular wavelength range. Furthermore, this anisotropic material also limits the application of the lens to the fractional Fourier transform (FRFT),⁷ which is widely used in image processing and other information systems.⁸ To indicate this limit, we consider the two-dimensional (2D) device for transverse electric (TE) or transverse magnetic (TM) waves. A conventional GRIN lens can have the refractive index distribution as $n(y) = n_0[1 - (1/2)\eta^2 y^2]$, where y is the radial distance from the optical axis and n_0 and η are the GRIN lens parameters.⁹ Under the paraxial approximation, if the lens thickness $b = \pi/(2\eta)$, the signal at the output facet becomes a Fourier transformed one of the input signal.⁹ According to the optically interpreted FRFT, the α -order FRFT ($0 \leq \alpha \leq 1$) can be physically defined as the

functional form of the output signal at αb from the input facet,⁷ which is located at the inner region of the lens. As the anisotropic unit block is constructed from different material layers,⁶ the system is also challenging for small-scale fabrication and thus the inner region of the lens is discrete to some degree. This discreteness will influence the signal detection precision in the inner region. Therefore, to promote the broadband and low-loss practical application of optical FRFT, where the traditional Fourier transform is viewed as a special case when $\alpha = 1$, an isotropic material is in great demand for such a transformation lens.

To achieve the isotropic transformation media, one can use the numerical method based on inverse Laplace's equation with sliding boundaries.¹⁰ For further application, it is better to get the transformation material in analytical form, such as conformal mapping in the complex plane.³ Here we propose a potentially more flexible alternative of this design, with which the space mapping can be obtained step by step directed by straightforward geometrical senses. To this end, the deformation view of the transformation optics is introduced, where the transformed material parameters can be expressed in a geometrical way¹¹ as

$$\begin{aligned} \epsilon' &= \epsilon_0 \text{diag} \left[\frac{\lambda_1}{\lambda_2 \lambda_3}, \frac{\lambda_2}{\lambda_1 \lambda_3}, \frac{\lambda_3}{\lambda_1 \lambda_2} \right] \\ \mu' &= \mu_0 \text{diag} \left[\frac{\lambda_1}{\lambda_2 \lambda_3}, \frac{\lambda_2}{\lambda_1 \lambda_3}, \frac{\lambda_3}{\lambda_1 \lambda_2} \right], \end{aligned} \quad (1)$$

where λ_1 , λ_2 , and λ_3 are the three principal stretches of a spatial element during space deformation, and ϵ' and μ' are the transformed permittivity and permeability, respectively. Equation (1) is established in the local principal system of the deformation. Instead of directly adjusting the explicit coordinate transformation expression, Eq. (1) suggests that one can adjust the principal stretches, which have very clear geometrical meaning, to manipulate the transformed material parameters.

Accordingly, our design should be divided into two steps, as shown in Fig. 1, by which the input facet of the conventional GRIN lens is compressed while the output facet remains the same.⁶ First, a rectangle ABCD is bent to a sector $A^I B^I C^I D^I$ with the side length $A^I D^I = b$ and the output facet size $A^I B^I = a$, both of which remain unchanged, where superscript I indicates the first-step transformation. At each point, there is only rescaling in the θ direction during the deformation, and this stretch can be easily obtained by comparing the arc length βr with its original length a , thus the principal stretches are

$$\lambda_\theta^I = \frac{\beta r}{a}, \quad \lambda_r^I = 1. \quad (2)$$

According to Eq. (1), this transformation will result in the anisotropic medium, as was shown in Ref. 6. Now, let us carry out the second-step transformation $r' = f(r)$, $\theta' = \theta$ in the polar co-ordinate system shown in Fig. 1(b) and 1(c), where the continuous function $f(r)$ is to be determined. This transformation will lead to principal stretches

$$\lambda_\theta^{II} = \frac{r' d\theta'}{r d\theta} = \frac{r'}{r}, \quad \lambda_r^{II} = \frac{dr'}{dr}, \quad (3)$$

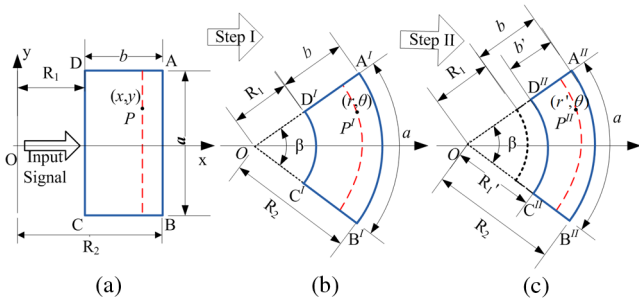


Fig. 1 Two-step transformation of the isotropic Fourier lens: (a) original space of the conventional rectangle-shaped GRIN lens; (b) space after the first-step transformation; (c) space after the second-step transformation.

where the superscript *II* indicates the second-step transformation. To obtain the isotropic transformation material, the total stretches in the $\hat{\theta}$ and \hat{r} directions should be equal, so that

$$\lambda_{\theta} = \lambda'_{\theta} \lambda''_{\theta} = \lambda_r = \lambda'_r \lambda''_r \equiv \lambda. \quad (4)$$

By inserting Eqs. (2) and (3) into Eq. (4), one has

$$\lambda = \frac{dr'}{dr} = \frac{\beta r'}{a}. \quad (5)$$

With the boundary condition that the output facet size is unchanged, i.e., $r'(r = R_2) = R_2$, the function $f(r)$ can be solved from Eq. (5) as

$$r' = f(r) = R_2 e^{\frac{\beta}{a}(r-R_2)}. \quad (6)$$

As there is no transformation in the \hat{z} direction, or $\lambda_z = 1$, the resulting material parameters, according to Eq. (1), will be $\epsilon'_r = \epsilon'_\theta = \epsilon_0$, $\mu'_r = \mu'_\theta = \mu_0$, $\epsilon'_z = (1/\lambda)^2 \epsilon_0$, and $\mu'_z = (1/\lambda)^2 \mu_0$.

Thus, the isotropic refractive index for TE or TM waves is $n'_r = n'_\theta = (1/\lambda)n$, where $n = \sqrt{\epsilon_0 \mu_0}$ is the refractive index of the conventional rectangle-shaped GRIN lens.

To validate the transformed material parameters, a numerical simulation was performed using the software COMSOL Multiphysics, where we set $\beta = 1$ radian and $R_2 = a = 3.5 \mu\text{m}$, $b = 3.0377 \mu\text{m}$, $n(y) = 1.5[1 - (1/2)\eta^2 y^2]$ with $\eta = 0.5171$, i.e., $b = \pi/(2\eta)$. The enhancement factor of the designed lens γ is the compression factor of the input boundary $1/\lambda(r' = R_1')$ ⁶ and can be obtained from Eqs. (5) and (6). In this example, $\gamma = 2.3819$. The simulation results are shown in Fig. 2, where the wavelength of the input TE wave is $0.15 \mu\text{m}$, and the wave is impinging on the input facet with aperture width d , therefore the rectangular aperture function is optically Fourier transformed to sinc function at the output facet. For the designed lens, we set $d = 0.3 \mu\text{m}$, shown in Fig. 2(b); for the conventional GRIN lens, we set $d = \gamma \times 0.3 \mu\text{m} = 0.7146 \mu\text{m}$, shown in Fig. 2(a). Owing to paraxial approximation, the widths of the output signals that are well matched with the ideal ones are about $1.6 \mu\text{m}$. It is clear that a narrower input signal in the designed lens can obtain the same effective output signal, shown in Fig. 2(e) as that in the conventional GRIN lens in Fig. 2(d) with a γ -times wider input signal; thus, a γ -times enhancement for the input bandwidth was achieved.⁶ Furthermore, we set d also equal to $0.3 \mu\text{m}$ for the conventional GRIN lens in Fig. 2(c) and checked its output signal $g(\kappa) \sim \text{sinc}(u)$, where κ denotes spatial frequency and $u = \pi d \kappa$.⁹ It can be shown that in the conventional lens if $u = \pi$, where the sinc function becomes zero as seen in Fig. 2(f), the corresponding u in the designed lens is about 2.38π , shown in Fig. 2(e), thus a greater amount (2.38 times) of spatial frequency is revealed in the latter.

The designed lens itself is an FRFT device because of its semigroup property.⁷ To obtain its α order FRFT, the

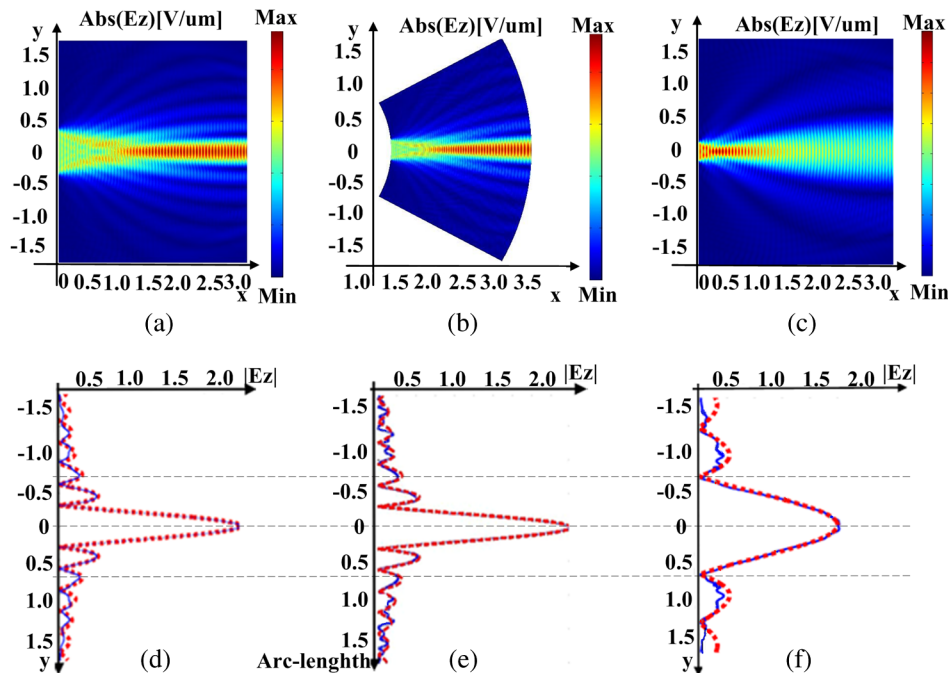


Fig. 2 Contour plots of the electric fields $|E_z|$ in the devices and the corresponding amplitude spectrum along the output facet. (a) and (d): conventional lens with $d = 0.7146$; (b) and (e): designed lens with $d = 0.3$; (c) and (f): conventional lens with $d = 0.3$. The blue solid lines in (d), (e) and (f) are the simulation results, while the red dotted lines are the ideal ones.

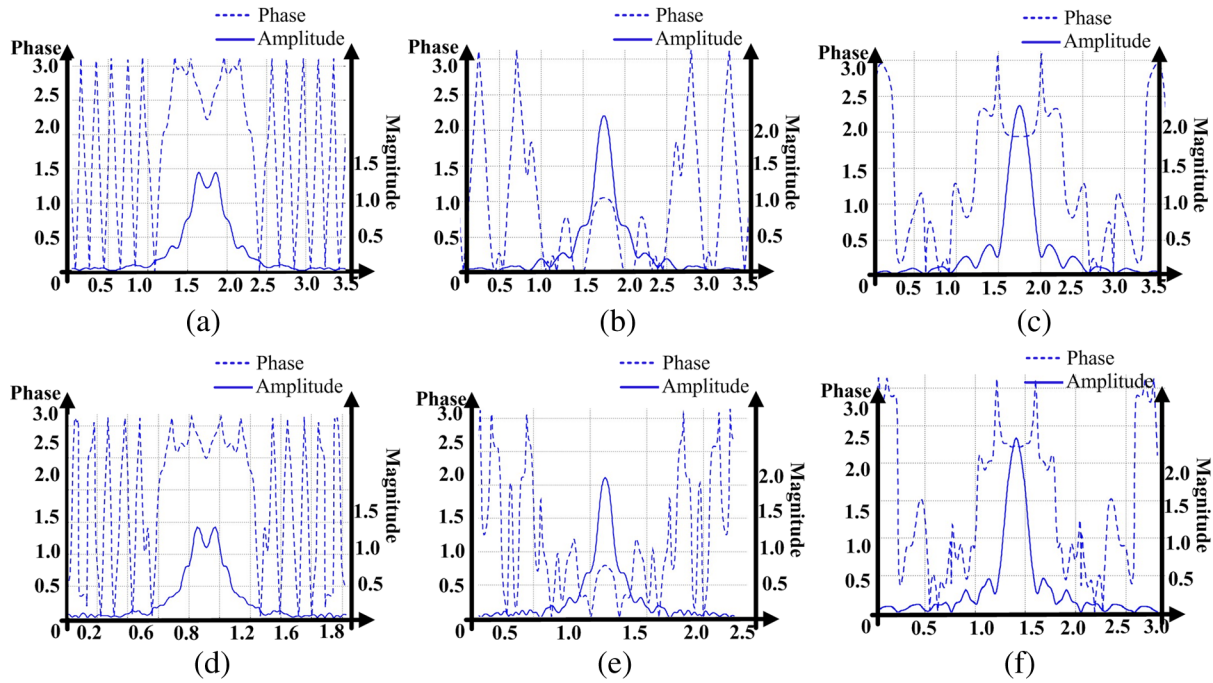


Fig. 3 Amplitude and phase spectra of FRFT results with different orders α . (a), (b), and (c): conventional lens with $\alpha = 0.25, 0.5,$ and $0.75,$ respectively; (d), (e), and (f) are the corresponding results in the designed lens.

detection line is usually located at ab' from the input facet. However, the FRFT result will be different from that of the conventional one with the same order α , because this detection location is not the transformation counterpart of the original one. The points at line $x = R_1 + ab$ in Fig. 1(a) are transformed to points at line $r' = f(R_1 + ab)$, not the line $r' = R_1' + ab'$ in Fig. 1(c), as shown in Eq. (6). Thus, according to the idea of transformation optics, to obtain the same FRFT results in the designed lens as those of the conventional one for the same order α , the detection location must be moved from the line $r' = R_1' + ab'$ to $r' = f(R_1 + ab)$. To validate the adjustment effects, FRFTs with $\alpha = 0.25, 0.5,$ and 0.75 were checked, respectively, in the same simulation environment as Fig. 2(a) and 2(b), and the results are shown in Fig. 3, where the compressed widths of the FRFT results in the designed lens have already been normalized for convenience of comparison. Only the results near the optical axis are considered according to the paraxial approximation. It is clear that the designed lens can provide almost the same FRFT results as that of the conventional lens for the same order. More demonstrations of the optical FRFT in conventional GRIN lens can be found in Ref. 12.

To conclude, keeping the principal stretches equal in the space mapping, an isotropic material can be designed for the Fourier lens that has an enhanced input spatial frequency bandwidth. The isotropic material, having important features like broadband and low loss, is also less discrete, and that helps the practical application of FRFT. More discussions on the deformation view of the transformation method can be found in Refs. 13–15. The clear geometrical sense provided by this view can help in optimizing more potential transformation media designs.

Acknowledgments

This work was supported by the National Natural Science Foundation of China (11172037) and Excellent Young Scholars Research Fund of Beijing Institute of Technology (2011YR0509).

References

1. A. Greenleaf, M. Lassas, and G. Uhlmann, "On non-uniqueness for Calderon's inverse problem," *Math. Res. Lett.* **10**(5–6), 685–693 (2003).
2. J. B. Pendry, D. Schurig, and D. R. Smith, "Controlling electromagnetic fields," *Science* **312**(5781), 1780–1782 (2006).
3. U. Leonhardt, "Optical conformal mapping," *Science* **312**(5781), 1777–1780 (2006).
4. H. Chen and C. T. Chan, "Acoustic cloaking in three dimensions using acoustic metamaterials," *Appl. Phys. Lett.* **91**(18), 183518 (2007).
5. J. Hu, Z. Chang, and G. K. Hu, "Approximate method for controlling solid elastic waves by transformation media," *Phys. Rev. B* **84**(20), 201101(R) (2011).
6. J. Li et al., "Designing the Fourier space with transformation optics," *Opt. Lett.* **34**(20), 3128–3130 (2009).
7. D. Mendlovic and H. M. Ozaktas, "Fractional Fourier transforms and their optical implement: I," *J. Opt. Soc. Am. A* **10**(9), 1875–1881 (1993).
8. R. Tao, F. Zhang, and Y. Wang, "Fractional power spectrum," *IEEE Trans. Sig. Process.* **56**(9), 4199–4206 (2008).
9. A. Yariv, *Optical Electronics*, 3rd ed., Holt Reinhart, New York (1985).
10. Z. Chang et al., "Design method for quasi-isotropic transformation materials based on inverse Laplace's equation with sliding boundaries," *Opt. Express* **18**(6), 6089–6096 (2010).
11. J. Hu, X. Zhou, and G. K. Hu, "Design method for electromagnetic cloak with arbitrary shape," *Opt. Express* **17**(3), 1308–1320 (2009).
12. H. M. Ozaktas and D. Mendlovic, "Fourier transforms of fractional order and their optical interpretation," *Opt. Commun.* **101**(3–4), 163–169 (1993).
13. J. Hu, X. Liu, and G. K. Hu, "Constraint condition on transformation relation for generalized acoustics," *Wave Motion* **50**(2), 170–179 (2013).
14. J. Hu and X. Y. Lu, "Determining the full transformation relations in the transformation method," *Appl. Phys. A* **109**(4), 971–977 (2012).
15. J. Hu, X. Zhou, and G. K. Hu, "Nonsingular two dimensional cloak of arbitrary shape," *Appl. Phys. Lett.* **95**(1), 011107 (2009).